



Rapid Electrochemical Synthesis and Solvatochromic Emission Behavior of Single Crystals of a Heteronuclear Platinum(II)-Copper(I) Complex

Yijia Liu¹ | Limin Zhang¹ | Yun Ma² | Pengfei She¹ | Wei Tang³ | Wai-Yeung Wong¹

¹Department of Applied Biology and Chemical Technology and Research Institute for Smart Energy, The Hong Kong Polytechnic University, Hung Hom, P. R. China | ²State Key Laboratory of Flexible Electronics (LoFE) & Institute of Advanced Materials (IAM). Nanjing University of Posts and Telecommunications (NUPT), Nanjing, P. R. China | ³Shenzhen Luojia New Material Technology Co. Ltd., Shenzhen, P. R. China

Correspondence: Yun Ma (iamyma@njupt.edu.cn) | Wai-Yeung Wong (wai-yeung.wong@polyu.edu.hk)

Received: 25 March 2025 | Revised: 24 May 2025 | Accepted: 8 June 2025

Funding: Wai-Yeung Wong acknowledges the financial support from the National Key R&D Program of China (2022YFE0104100), the National Natural Science Foundation of China (52073242), the RGC Senior Research Fellowship Scheme (SRFS2021-5S01) and General Research Fund (PolyU 15301922), the Research Institute for Smart Energy (CDAQ), the Research Centre for Nanoscience and Nanotechnology (CE2H), the Research Centre for Carbon-Strategic Catalysis (CE01 and CE2L) and Miss Clarea Au for the Endowed Professorship in Energy (847S).

Keywords: anti-counterfeiting | electrochemical synthesis | heterometallic complexes | photoluminescence | solvatochromism

ABSTRACT

In this study, we present a novel multicomponent self-assembly approach that offers good potential for crafting heterometallic complexes with exceptional constitutional control. This method generates metal ions from a sacrificial anode by using an electric field, which then coordinates with a metal complex precursor. As a proof-of-concept demonstration, we successfully synthesized single crystals of a heterometallic platinum(II)-copper(I) (Pt[II]-Cu[I]) complex at an exceptionally rapid rate within 30 s by applying a voltage to an acetonitrile solution of $[Pt(ppy)(CN)_2]^-Bu_4N^+$, using copper foil as the anode. Intriguingly, by finely adjusting the intensity and duration of the electric field, we achieved a variety of supramolecular structures, spanning from spherical to rod-like and even flower-like morphologies. Additionally, we found that the photoluminescence property of the resultant crystal can be reversibly shifted among green, orange, and cyan by merely altering the solvent environment. Finally, the crafted heterometallic Pt(II)-Cu(I) complex has shown great promise in advanced anti-counterfeiting applications.

1 | Introduction

Heterometallic complexes, composed of two or more different metal ions, are at the forefront of coordination chemistry and materials science due to their unique and adjustable properties [1–5]. By integrating the characteristics of multiple metal ions, these complexes provide synergistic properties and multifunctionality that cannot be achieved with individual homometallic components [6–9]. As a result, they hold great potential for diverse areas such as catalysis, biomedical applications, and information science. For instance, when a light-absorbing metal

group is paired with an emissive metal unit, it allows for the development of efficient energy transfer systems [10–12]. These systems can be used as luminescent materials or anticounterfeiting tags [13–17]. Additionally, incorporating multiple metal centers offers good avenues to precisely tune the magnetic properties, from single-molecule magnet behavior to magnetic refrigeration property [18–21].

However, despite the great promise of heterometallic systems, the synthesis of high-quality heterometallic complexes with controlled composition and structure remains a persistent challenge.

This is an open access article under the terms of the Creative Commons Attribution License, which permits use, distribution and reproduction in any medium, provided the original work is properly cited.

© 2025 The Author(s). Aggregate published by SCUT, AIEI and John Wiley & Sons Australia, Ltd.

One major difficulty is the mismatch between metal centers in terms of redox potential, coordination geometry preference, and solubility in solvents. These differences make it hard to achieve evenly mixed and distributed metal centers, which often result in phase segregation or uncontrolled precipitation. Moreover, traditional synthesis methods for these heterometallic complexes often require multiple precursors in a self-assembly reaction. This introduces additional equilibria from potential metal and ligand exchange reactions, resulting in the formation of closely related structures. Single-crystal X-ray diffraction (SC-XRD) analysis stands as a formidable tool for unraveling intricate structures. However, its effectiveness is frequently curtailed by the challenge of obtaining high-quality single crystals (SCs). Traditional synthesis approaches usually involve harsh reaction conditions and long reaction times, hindering the generation of SCs suitable for detailed structural analysis. Consequently, the efficient production of high-quality SCs becomes a formidable task [22-26].

Considering the limitations of conventional synthetic methods, it is imperative to develop alternative approaches for the preparation of heterometallic complexes. Given the proven success of electrochemical synthesis in generating diverse small organic molecules/metal oxides and orchestrating the formation of such compounds at the nanoscale, we are inclined to believe that this method holds great promise for the rapid and mild production of high-quality SCs [27, 28]. By applying a controlled electrical potential during synthesis, it is possible to precisely modulate parameters like metal ion diffusion rates, nucleation processes, and crystallite development pathways. This electrochemical control opens ways to metastable coordination complexes and nano/microstructures, which are challenging to achieve with conventional reaction methods. Furthermore, the electric field-assisted method may enable in situ crystal engineering, promoting the fast growth of high-quality SCs even in systems that typically resist dissolution. This advancement paves the way for analyzing new metal complexes using the XRD technique.

Here, we demonstrate the possibility of an electric fieldguided method in assembling novel heterometallic platinum(II)copper(I) (Pt[II]-Cu[I]) complexes with tunable photoluminescence (PL) properties. We employed the anionic part of [Pt(ppy)(CN)₂]⁻Bu₄N⁺ as a precursor because its cyano ligand is recognized for its exceptional ability to form ordered assemblies with various cations from the main group, transition metal, and rare-earth elements. During the process, copper foil acts as the sacrificial anode, releasing copper ions when the electric field is applied. These metal ions then coordinate with the nitrogen atom of the cyanide ligand in the Pt(II) complex precursor, resulting in a quadrangular ring structure. Notably, we obtained SCs at an exceptionally rapid rate within 30 s for in-depth analysis. By adjusting electric field variables such as voltage and duration, we crafted diverse Pt(II)-Cu(I) structures, from spheres and rods to intricate flower-like superstructures. Structural analysis unveiled a square planar geometry, underscoring the capability of the electric field to produce outcomes unattainable via traditional methods. We further discerned structure-function correlations by linking morphologies to specific emission colors (cyan, green, and orange) under varying solvent conditions. Overall, this research emphasizes the transformative potential of an external electric field in refining the synthesis of complex heterometallic systems by offering unparalleled molecular assembly control. The insights garnered lay the groundwork for the production of switchable emissive materials, anti-counterfeiting labels, and sensing platforms.

2 | Results and Discussion

The synthesis of the precursor $[Pt(ppy)(CN)_2]^-Bu_4N^+$ is shown in the supporting information. Figure 1 illustrates the experimental setup for the Pt(II)-Cu(I) complex synthesis, using acetonitrile (ACN) as the solvent. In this setup, the Pt wire functions as an inert cathode, while the copper foil acts as a sacrificial anode to release Cu(I) cations. Under a potentiostatic electric field, these Cu(I) cations coordinate with the anionic platinum(II) complex, resulting in a neutral, square-like tetranuclear Pt(II)-Cu(I) complex. Following this electric field-assisted assembly, SCs are formed directly within the electrolytic cell, suitable for XRD analysis.

The morphological characteristics of the morphology-controlled Pt(II)-Cu(I) complex under varying electric fields were systematically examined by scanning electron microscopy (SEM). As evidenced in Figure 2a,f, at an applied potential of 0.1 V, owing to the influence of surface energy, the embryonic crystal nuclei that emerge during the initial stages of Pt(II)-Cu(I) complex aggregation manifest as spherical entities with a smooth surface, exhibiting a diameter spanning the range of approximately 300-500 nm. With an increase in the applied potential gradient, there is an accelerated generation of Cu⁺ ions around the anode. These ions promptly coordinate with the Pt(II) precursor in the solution, resulting in the formation of an increased concentration of Pt(II)-Cu(I) complex species. Evidently, these newly formed molecule exhibits a propensity to irregularly affix themselves to the spherical nuclei. This phenomenon leads to the development of a quasi-spherical structure with a protruding surface similar in size to the previous ones (300-500 nm). Upon reaching a voltage of 1 V, an augmentation in the concentration of the Pt(II)-Cu(I) complex occurs, leading to a partial establishment of an orderly arrangement. This induces the growth of numerous systematically aligned rod-like structures around a central core. Simultaneously, the disparate energy profiles and structural attributes of distinct crystal facets lead to differential growth rates along specific directions, ultimately resulting in the formation of a "bowtie-shaped" aggregate morphology with a length of about 25 µm.

After this, with the incremental increase of voltage, a notable propensity is discerned whereby molecules tend to adopt the most energetically favorable configuration, promoting a progressive shift towards regular and organized structures. Consequently, aggregates growing predominantly in the dominant direction progressively supplant other comparatively disordered branching structures and coalesce into a unified crystal structure. Figure 2c-f illustrates the dynamic morphological progression of this process, with the supramolecular structure transforming from "bowtie-shaped" to "bar-shaped". As the voltage increases, the aggregate's endpoints gradually come together, resulting in the formation of a flat and wide rod-like crystal structure when the electrical potential difference reaches 3 V. It is worth noting

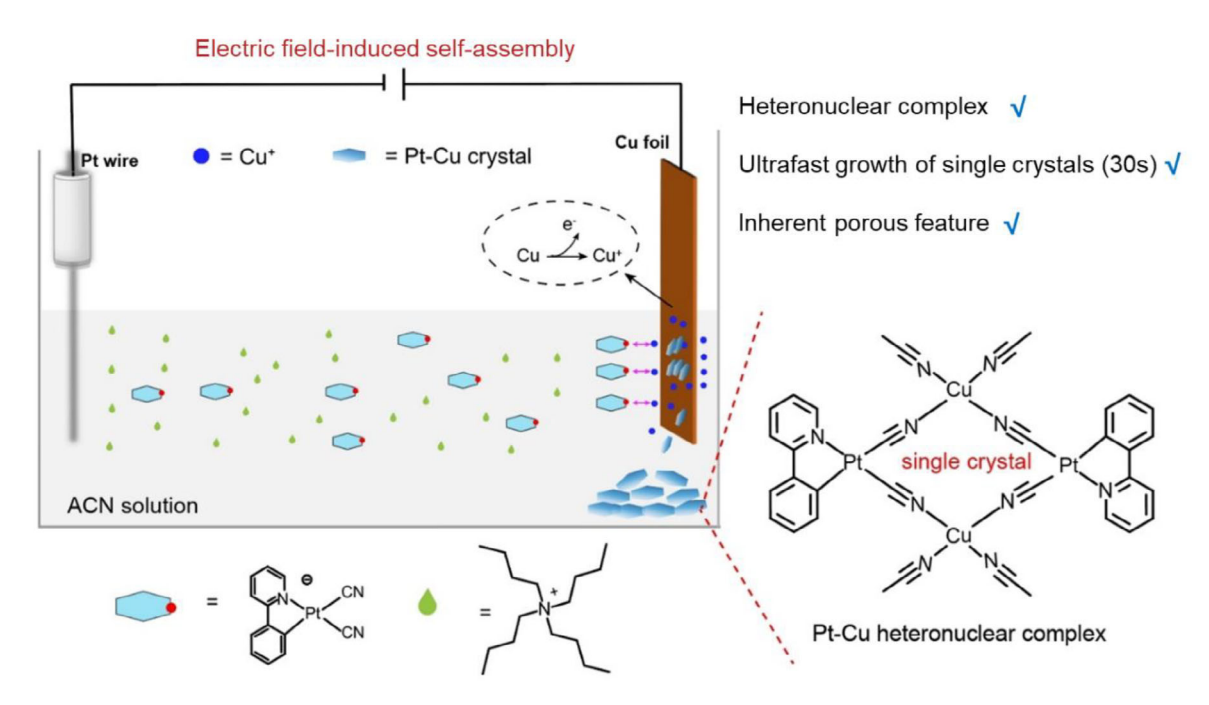


FIGURE 1 | Schematic design of the ultrafast growth of single crystals of the platinum(II)-copper(I) (Pt[II]-Cu[I]) heteronuclear complex by electric field-induced self-assembly.

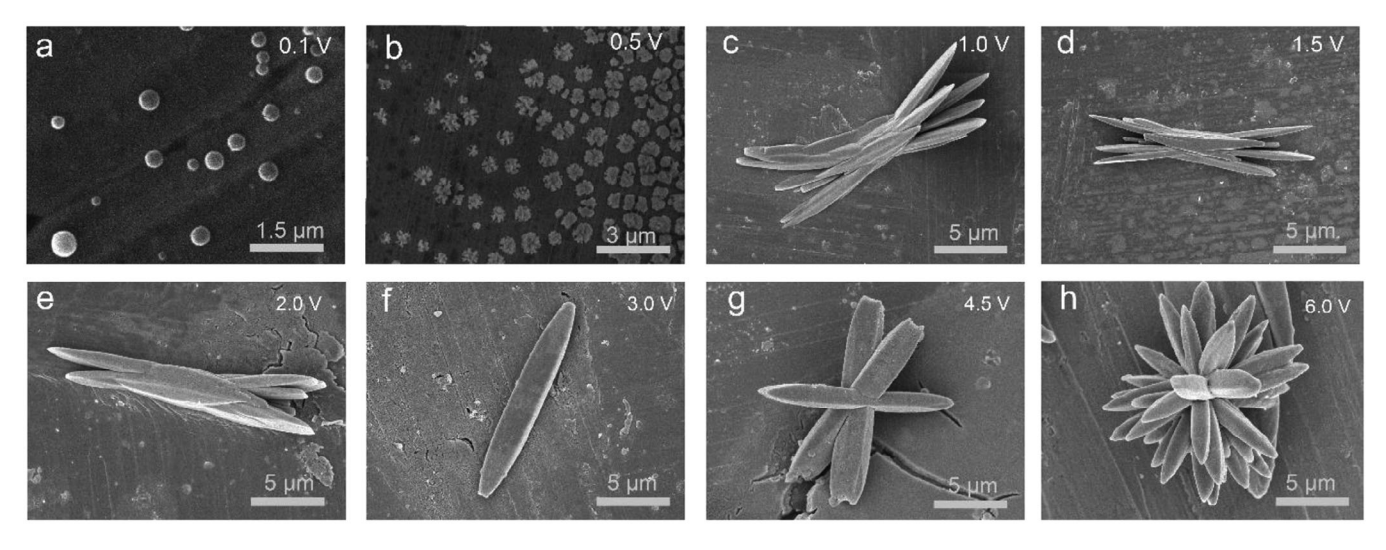


FIGURE 2 | Scanning electron microscopy (SEM) images prepared in the acetonitrile (ACN) solution of the platinum(II)-copper(I) (Pt[II]-Cu[I]) complex $(1 \times 10^{-4} \text{ M})$ by applying different voltages (0.1-6.0 V) for 60 s.

that within this electric field condition, we achieved the direct acquisition of SCs of Pt(II)-Cu(I) complex suitable for SC-XRD analysis through the electric field-induced assembly process. The data were collected at 297 K and the complex crystallized in the monoclinic $P2_1/c$ space group, with its structure illustrated in Figure 3. In the structure, copper ions coordinating with the Pt(II) precursor form the neutral square-like tetranuclear Pt(II)-Cu(I) complex. Notably, the packing pattern of the crystal shows a $\pi \cdots \pi$ interaction at about 3.6 Å, but without any Pt···Pt interaction. The crystallographic data are shown in Table S3.

With a further increase in voltage, the Cu(I) generation rate is accelerated. Since the reaction is essentially governed by the concentration of copper ions, higher concentrations lead

to reduced selectivity in the supramolecular formation. Consequently, stronger connections form highly branched and ordered rod-like supramolecular structures. As demonstrated in Figure 2f-h, there is a gradual increase in the organization of branches when the voltage ranges from 1 to 6 V, culminating in the formation of a flower-like supramolecular structure at a potential difference of 6 V. These findings underscore the capability of the electric field to enable the synthesis of the metal complex with controllable morphologies, attaining regular intermediate morphologies at various stages of supramolecular formation.

To validate the crystalline integrity of the Pt(II)-Cu(I) complexes synthesized under varying electric fields, powder XRD (PXRD) analysis was performed on samples obtained at 0.75 V, 1 V, 3 V, and

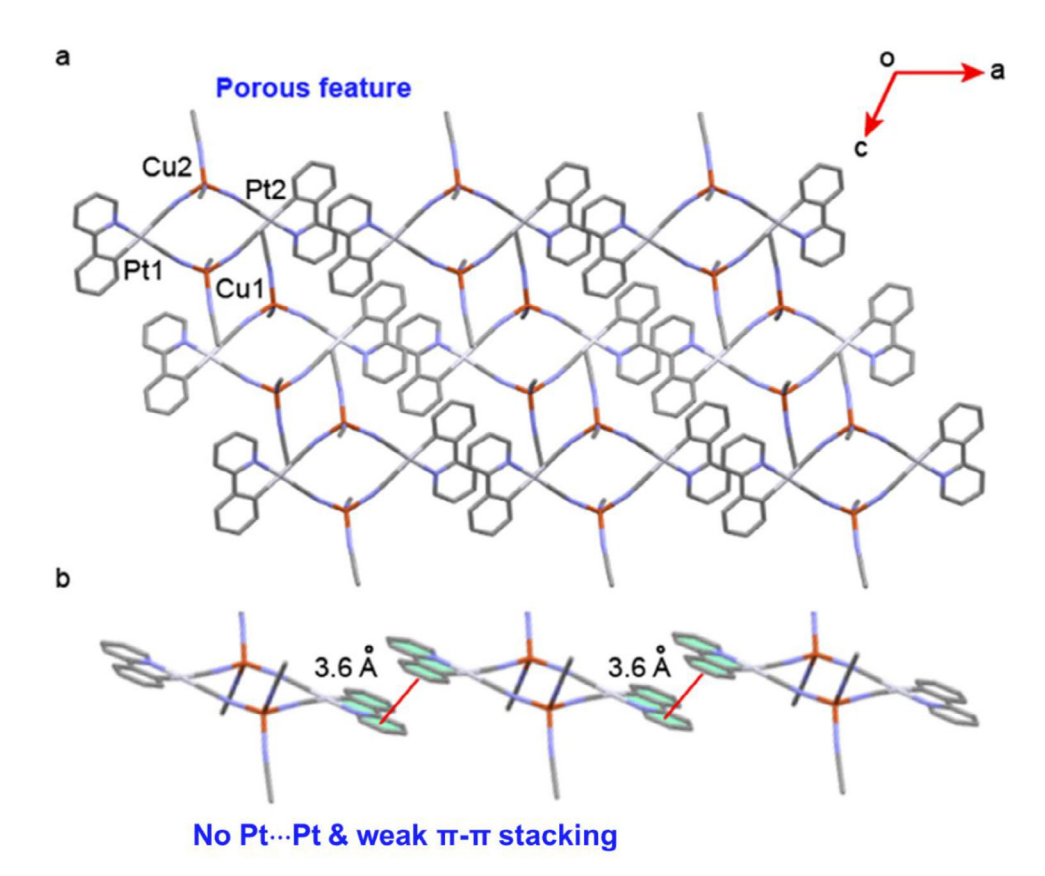


FIGURE 3 | Crystal structure and packing mode of the Pt(II)-Cu(I) complex.

6 V (Figure S4). All experimental patterns align closely with the simulated PXRD derived from the single-crystal structure of the Pt(II)-Cu(I) complex, confirming that the distinct morphologies observed in SEM share an identical crystalline lattice, regardless of the applied voltage. The minor intensity variations in PXRD patterns likely arise from the differences in crystallite orientation or size distribution during electric field-driven assembly, rather than structural divergence.

The emission behavior for the Pt(II)-Cu(I) complex in the dimethyl sulfoxide (DMSO)/water mixture was systematically investigated. As illustrated in Figure 4a, in a pristine DMSO solution of Pt(II)-Cu(I) complex, there is a weak emission, featuring two distinct peaks at approximately 480 and 510 nm when excited at a wavelength of 365 nm. After the introduction of the poor solvent, water, into the DMSO solution of the Pt(II)-Cu(I) complex, a gradual enhancement in emission intensity is observed. This phenomenon can be attributed to the gradual separation of the complex induced by the addition of a small quantity of water, resulting in the formation of minuscule crystals. These small crystals, present in the coordinative DMSO environment, exhibit a slightly stronger green emission when interacting with DMSO. With an escalating proportion of the poor solvent reaching 50%, a novel broad emission band emerged at approximately 580 nm. Because aggregate formation in the system outpaced the establishment of a complete interaction with the solvent, this results in the observed characteristic orange emission associated with the Pt(II)-Cu(I) molecule. Nonetheless, after a period of time, these aggregates acquire sufficient time to establish a comprehensive interaction with the solvent, leading to the system stabilizing into a state of green emission. As the water volume fraction incrementally rises to 70%, the rate of aggregate formation is further accelerated, culminating in its maximum intensity within the emission band at around 580 nm. With a progressive increase in the percentage of a poor solvent, a greater number of larger aggregates are rapidly formed. Due to their increased size, these aggregates precipitate more swiftly, leading to a reduction in the emission intensity of the system. This trend becomes particularly pronounced with a higher water content.

To elucidate the origin of the solvatochromic emission behavior, we investigated the UV-Vis absorption spectra of the Pt(II)-Cu(I) complex in DMSO/H₂O mixtures (Figure S5). Two prominent absorption bands are observed at approximately 310 nm and 380 nm, corresponding to the $\pi \rightarrow \pi^*$ transitions of the cyclometalated ppy ligand and metal-to-ligand charge transfer (MLCT) transitions involving the Pt-Cu framework, respectively. As the water content increases (0%-90%), both absorption bands exhibit a progressive blue shift ($\Delta\lambda \approx 8$ –12 nm), indicative of intermolecular π - π stacking interactions characteristic of H-aggregation. This hypsochromic shift aligns with the formation of ordered aggregates, where the parallel alignment of chromophores elevates the energy of the ground-to-excited state transition. Notably, despite the blue-shifted absorption, the emission spectra (Figure 4a) display a concomitant red shift (510 nm \rightarrow 600 nm) in high-water-content mixtures. This apparent dichotomy arises from aggregation-induced stabilization of a lower-energy emissive state following the initial excitation to the H-aggregate excited state. The restricted intramolecular motion in the aggregated phase suppresses non-radiative decay pathways,

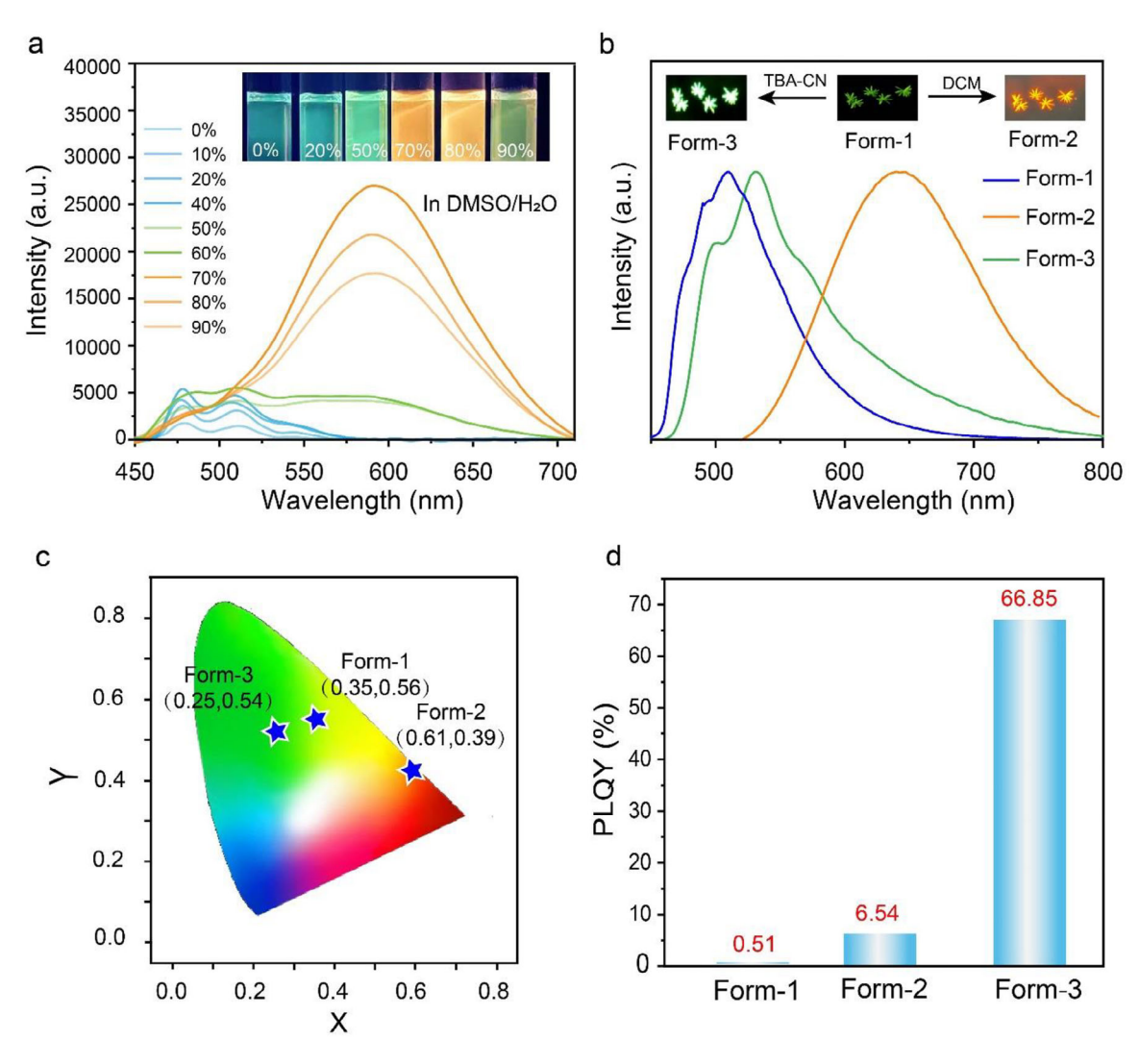


FIGURE 4 | (a) Emission spectra with emission photos collected at different ratios of dimethyl sulfoxide (DMSO)-water volume. As the water content increases from 0% to 90%, the emission changes from green to orange. Ultraviolet (UV) light ($\lambda_{ex} = 365$ nm). Concentration: 1×10^{-5} M. (b) Emission spectra of the three forms of crystals in the solid state. (c) Commission Internationale de l'Éclairage graph of the emission of crystals of the Pt(II)-Cu(I) complex. (d) PLQY of three different forms of crystals.

enhancing radiative recombination and yielding the observed aggregation-induced emission (AIE) behavior.

To definitively establish the role of Cu(I) in solvatochromic behavior, control experiments with the monometallic Pt(II) precursor [Pt(ppy)(CN)₂]^Bu₄N⁺ were conducted. The precursor exhibits a fixed ligand-centered (LC) emission at $\lambda_{\rm max}\approx 490$ nm across all solvents, demonstrating no solvatochromic response. In DMSO/H₂O mixtures, the Pt(II) precursor's emission intensity diminishes with increasing water content (Figure S8), while the Pt(II)-Cu(I) complex exhibits aggregation-induced emission enhancement and a redshift to $\lambda_{\rm max}\approx 600$ nm (Figure 4a). This stark contrast underscores Cu(I)'s critical role in enabling MLCT/LLCT transitions and AIE behavior, highlighting the synergistic effects of the heterometallic framework.

Next, the photophysical properties of the Pt(II)-Cu(I) complex in the solid state have been studied. We observed intriguing solvatochromic emission behavior of the Pt(II)-Cu(I) complex. Despite distinct morphologies (spherical, rod-like, flower-like;

Figure 2), all Pt(II)-Cu(I) aggregates adopt identical emission profiles after solvent treatment. During the electric field-induced assembly process under a variety of potential differences, the initially formed aggregates, generated near the copper electrode within the electrolyte, exhibit an orange emission when excited with a wavelength of 365 nm. This emission possibly arises from individual complex molecules within aggregates that have not yet had the opportunity to establish a stable interaction with a coordinative solvent. In contrast, the supramolecular structures that orderly assembled on the electrode surface emitted green light. This emission may be attributed to the stable state of interaction between the crystals and a coordinative electrolyte ACN solvent.

Subsequently, we conducted a comprehensive examination of the photophysical properties of the Pt(II)-Cu(I) complex. As depicted in Figure 4b, the Pt(II)-Cu(I) crystal, synthesized from an ACN solution, exhibits a distinctive emission, likely attributed to the influence of the coordinated solvent environment on the crystal's properties. When excited at 365 nm and at room temperature, this

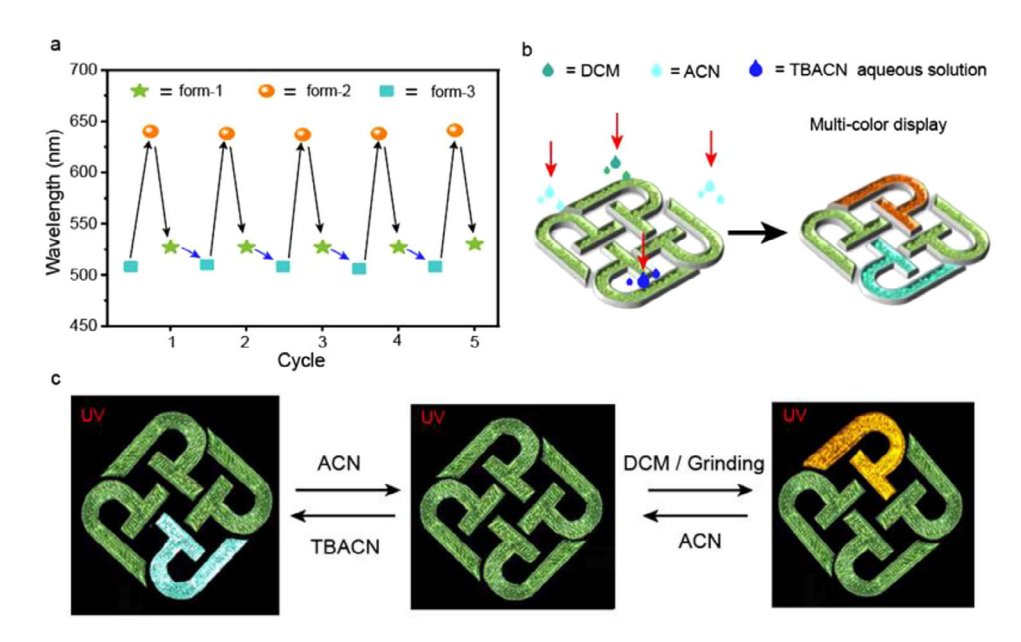


FIGURE 5 (a) Five cycles of emission wavelength variations measured after adding the corresponding solvents. (b, c) Illustration of the information encryption of Pt(II)-Cu(I) crystal using the dichloromethane (DCM), acetonitrile (ACN), and tetrabutylammonium cyanide (TBACN) aqueous solution. (c) Photographs of the Pt(II)-Cu(I) crystal before and after adding different solvents.

crystal emits a green light, characterized by a maximum emission wavelength (λ_{max}) of 530 nm, accompanied by a quantum yield (Φ_{em}) of 0.51% and an emission lifetime (τ) of 4.75 µs. This crystal variant is herein denoted as form-1. When form-1 is exposed to non-coordinating solvents such as dichloromethane, acetone, chloroform, chlorobenzene, n-hexane, etc., it undergoes a disruption of its prior environment of coordinative solvent. This alteration results in the compound exhibiting its intrinsic emission, characterized by a pronounced redshift in the maximum emission wavelength, extending by approximately 110 nm to 640 nm, accompanied by a shift in the emission color from green to orange. This altered form is referred to as form-2 and possesses a quantum yield (Φ_{em}) of 6.54% and an emission lifetime (τ) of 5.16 µs. Form-2 can also be achieved through mechanical grinding, thereby disrupting the coordinative solvent environment in form-1. This process can be effectively reversed by subjecting form-2 to ACN, facilitating the crystal's re-engagement with the coordinating solvent. Furthermore, exposure of form-2 to various solvents possessing coordination capabilities yields varying degrees of blue-shifted emissions, the specifics of which are summarized in Table S2 for reference.

To elucidate the transition character in the ground and triplet states of the Pt(II)-Cu(I) complex, density functional theory (DFT) calculations based on the SC were performed (Figure S10). The emission characteristics of the complex are ascribed to a synergistic interplay between MLCT and LC transitions. The observed emission is potentially linked to an excited-state energy transition from LC to MLCT processes. The orange emission is likely associated with the MLCT process, and the involvement of coordinating solvents elevates the energy of the MLCT state, thereby inducing a blue shift in the characteristic LC transition [29].

Additionally, when exposed to an aqueous solution of tetrabuty-lammonium cyanide (TBA·CN), tetrabutylammonium cyanate

(TBA·OCN) or tetrabutylammonium rhodanide (TBA·SCN) (concentration of 10 mg/mL), C≡N groups with superior coordination ability amplify the green emission of form-1, yielding λ_{max} = 500 nm, $\Phi_{\rm em}$ = 66.85%, and τ = 12.48 μ m. Furthermore, form-1 and form-2 can be regenerated from form-3 using an appropriate processing method, indicating complete reversibility in the emission color conversion among the three forms. The excitation and emission spectra for form-1, form-2, and form-3 in the solid state are depicted in Figure 4, while Table S1 provides a summary of the phosphor lifetime and quantum yield, with the corresponding spectrum displayed in Figure S2. Remarkably, the crystal of Pt(II)-Cu(I) complex exhibits the capacity for further chemical transformation, facilitating a direct conversion from crystal to crystal. When a Pt(II)-Cu(I) crystal is exposed to an ammonia atmosphere for a duration of 48 h, it undergoes a singlecrystal to single-crystal transformation, ultimately resulting in the formation of a non-emissive three-nucleated Pt(II)-Cu(II)-NH₃ crystal (see Figure S11 and Table S3 for crystal structure and reaction detail). This transformation involves the replacement of the two ligand molecules attached to a Cu atom in the Pt(II)-Cu(I) complex by three ammonia molecules, accompanied by the opening of the cyclometalated molecule's ring due to the loss of a Cu atom. This process involves the oxidation of copper from a valent state of +1 to a valent state of +2, with the entire molecule maintaining electrical neutrality.

The distinct excitation spectra of Form-1, Form-2, and Form-3 in the solid state (Figure S9) further corroborate the environment-dependent electronic states. Form-1 exhibits a sharp excitation maximum at 380–400 nm, consistent with its green emission ($\lambda_{\rm em}=530$ nm) under coordinating solvent conditions. In contrast, Form-2 shows a broadened, red-shifted excitation band (450–480 nm), aligning with its orange emission ($\lambda_{\rm em}=640$ nm) in non-coordinating environments. Form-3, stabilized by strong anion coordination (e.g., CN⁻), displays a blue-shifted excitation profile (360–380 nm) and cyan emission ($\lambda_{\rm em}=500$ nm).

SC-XRD analyses of Form-1, Form-2, and Form-3 confirm that all three polymorphs adopt an identical square-planar Pt(II)-Cu(I) tetranuclear core structure. Critical structural parameters and ligand coordination geometries remain invariant across the three forms (see Tables S4–S7). Subtle variations in intermolecular packing arise exclusively from solvent-coordination-induced lattice adjustments, as evidenced by crystallographic refinements. Crucially, these packing modifications do not perturb the heterometallic framework's electronic structure. The distinct emission maxima (Form-1: 530 nm, Form-2: 640 nm, and Form-3: 500 nm) are therefore attributed to solvent- or treatment-induced electronic state perturbations—not structural reorganization of the heterometallic core—as confirmed by invariant Pt–Cu bond lengths in SC-XRD analyses (Tables S3–S7).

The photostability and reversibility of the complex in three forms are investigated. As shown in Figure 5a, the emission intensity and maximum wavelength of these three crystals remained almost unchanged after continuous irradiation with UV light (365 nm) for 120 min. Also, the maximum emission of the crystals can be repeatedly manipulated between 500, 530, and 640 nm by exposing the crystals to specific solvents. After five cycles, their emission wavelength shows no degradation for each form. This excellent photostability and reversibility for all three forms indicate that the Pt(II)-Cu(I) complex is suitable for the optical anti-counterfeiting application [15].

The Pt(II)-Cu(I) complex shows a significant stimuli-responsive PL behavior, which meets the above security requirements. As shown in Figure 5b,c, the Pt(II)-Cu(I) complex was used as the solid ink to fill up the pattern of the PolyU logo. Under the 365 nm UV light, the emission color of the logo is green (form-1). By adding dichloromethane or acetone, chlorobenzene, o-dichlorobenzene, and chloroform, the emission color changes to orange (form-2) and cyan (form 3) when the added solvent is an aqueous solution of TBA·CN, TBA·OCN, or TBA·SCN. In particular, solvents can be added to different parts of the logo independently, indicating that the color of each part can be changed individually. This result demonstrates the potential of such Pt(II)-Cu(I) complex in anti-counterfeiting applications since the security of the produced tag is greatly enhanced due to the controllable change of the PL colors.

3 | Conclusion

In conclusion, our research has demonstrated a pioneering approach to the in-situ and ultrafast synthesis of a heterometallic Pt(II)-Cu(I) complex which can exist in various supramolecular nano/microstructures through the application of an electric field. The photophysical properties of this complex were found to exhibit intriguing solvent-dependent emission behavior, offering potential applications in luminescence tagging and anticounterfeiting technologies. This work opens up new avenues for the controlled assembly of functional materials with tailored supramolecular morphologically structures, driven by the external electric field. The ability to precisely modulate the assembly process and achieve diverse supramolecular structures has significant implications for the development of innovative functional materials and provides insights into molecular interactions across scientific disciplines.

CCDC-2423203 and 2423205 contain the supplementary crystallographic data for this paper. These data can be obtained free of charge from The Cambridge Crystallographic Data Centre via www.ccdc.cam.ac.uk/data_request/cif.

Acknowledgments

Wai-Yeung Wong acknowledges the financial support from the National Key R&D Program of China (2022YFE0104100), the National Natural Science Foundation of China (52073242), the RGC Senior Research Fellowship Scheme (SRFS2021-5S01) and General Research Fund (PolyU 15301922), the Research Institute for Smart Energy (CDAQ), the Research Centre for Nanoscience and Nanotechnology (CE2H), and the Research Centre for Carbon-Strategic Catalysis (CE01 and CE2L) and Miss Clarea Au for the Endowed Professorship in Energy (847S).

Conflicts of Interest

The authors declare no conflicts of interest.

References

- 1. S. A. Hua, M. C. Cheng, C. H. Chen, and S. M. Peng, "From Homonuclear Metal String Complexes to Heteronuclear Metal String Complexes," *European Journal of Inorganic Chemistry* no. 15 (2015): 2510–2523.
- 2. Q. Wang, H. Xiao, Y. Wu, Z. Y. Wang, D. S. Zheng, and Z. N. Chen, "From Homonuclear to Heteronuclear: A Viable Strategy to Promote and Modulate Phosphorescence," *Chemical Communications* 56, no. 73 (2020): 10607–10620.
- 3. Z. Chen, N. Zhao, Y. Fan, and J. Ni, "Luminescent Groups 10 and 11 Heteropolynuclear Complexes Based on Thiolate or Alkynyl Ligands," *Coordination Chemistry Reviews* 253, no. 1–2 (2009): 1–20.
- 4. Z. Li, H. Chen, B. Li, et al., "Photoresponsive Luminescent Polymeric Hydrogels for Reversible Information Encryption and Decryption," *Advanced Science* 6, no. 21 (2019): 1901529.
- 5. S. F. Rice, S. J. Milder, H. B. Gray, R. A. Goldbeck, and D. S. Kliger, "Photophysical Properties of the Lowest Electronic Excited States of Binuclear Rhodium(I) Isocyanide Complexes," *Coordination Chemistry Reviews* 43 (1982): 349–354.
- 6. V. W. Yam, V. K. Au, and S. Y. Leung, "Light-Emitting Self-Assembled Materials Based on d8 and d10 Transition Metal Complexes," *Chemical Reviews* 115, no. 15 (2015): 7589–7728.
- 7. Z. Y. Wang, L. Y. Zhang, L. J. Xu, L. X. Shi, J. Y. Wang, and Z. N. Chen, "Elaborate Design of d8–d10 Heteronuclear Phosphors for Ultrahigh-Efficiency Solution-Processed Organic Light-Emitting Diodes," *ACS Applied Materials & Interfaces* 13, no. 12 (2021): 14433–14439.
- 8. M. W. Cooke and G. S. Hanan, "Luminescent Polynuclear Assemblies," Chemical Society Reviews 36, no. 9 (2007): 1466–1476.
- 9. S. Chakraborty and G. R. Newkome, "Terpyridine-based Metallosupramolecular Constructs: Tailored Monomers to Precise 2D-Motifs and 3D-Metallocages," *Chemical Society Reviews* 47, no. 11 (2018): 3991–4016.
- 10. J. I. Deneff, K. S. Butler, L. E. S. Rohwer, et al., "Encoding Multilayer Complexity in Anti-Counterfeiting Heterometallic MOF-Based Optical Tags," *Angewandte Chemie International Edition* 60, no. 3 (2021): 1203–1211.
- 11. Y. Ai, Y. Li, M. H. Chan, G. Xiao, B. Zou, and V. W. W. Yam, "Realization of Distinct Mechano- and Piezochromic Behaviors via Alkoxy Chain Length-Modulated Phosphorescent Properties and Multidimensional Self-Assembly Structures of Dinuclear Platinum(II) Complexes," *Journal of the American Chemical Society* 143, no. 28 (2021): 10659–10667.
- 12. G. Huang, Y. Jiang, S. Yang, B. S. Li, and B. Z. Tang, "Multistimuli Response and Polymorphism of a Novel Tetraphenylethylene Derivative," *Advanced Functional Materials* 29, no. 16 (2019): 1900516.

- 13. L. M. C. Luong, M. A. Malwitz, V. Moshayedi, M. M. Olmstead, and A. L. Balch, "Role of Anions and Mixtures of Anions on the Thermochromism, Vapochromism, and Polymorph Formation of Luminescent Crystals of a Single Cation, [(C 6 H 11 NC) 2 Au] +," *Journal of the American Chemical Society* 142, no. 12 (2020): 5689–5701.
- 14. J. Liu, H. Rijckaert, M. Zeng, et al., "Simultaneously Excited Downshifting/Upconversion Luminescence From Lanthanide-Doped Core/Shell Fluoride Nanoparticles for Multimode Anticounterfeiting," *Advanced Functional Materials* 28, no. 17 (2018): 1707365.
- 15. A. K. Yetisen, I. Naydenova, F. da Cruz Vasconcellos, J. Blyth, and C. R. Lowe, "Holographic Sensors: Three-Dimensional Analyte-Sensitive Nanostructures and Their Applications," *Chemical Reviews* 114, no. 20 (2014): 10654–10696.
- 16. X. Yu, H. Zhang, and J. Yu, "Luminescence Anti-Counterfeiting: From Elementary to Advanced," *Aggregate* 2, no. 1 (2021): 20–34.
- 17. J. Li, K. Chen, J. Wei, et al., "Reversible on–Off Switching of Excitation-Wavelength-Dependent Emission of a Phosphorescent Soft Salt Based on Platinum(II) Complexes," *Journal of the American Chemical Society* 143, no. 43 (2021): 18317–18324.
- 18. V. A. Milway, F. Tuna, A. R. Farrell, L. E. Sharp, S. Parsons, and M. Murrie, "Directed Synthesis of {Mn 18 Cu 6 } Heterometallic Complexes," *Angewandte Chemie International Edition* 52, no. 7 (2013): 1949–1952.
- 19. V. W. W. Yam and A. S. Law, "Luminescent d8 Metal Complexes of Platinum(II) and Gold(III): From Photophysics to Photofunctional Materials and Probes," *Coordination Chemistry Reviews* 414 (2020): 213298.
- 20. K. Chan, C. Y. S. Chung, and V. W. W. Yam, "Parallel Folding Topology-selective Label-free Detection and Monitoring of Conformational and Topological Changes of Different G-quadruplex DNAs by Emission Spectral Changes via FRET of mPPE-Ala–Pt(ii) Complex Ensemble," *Chemical Science* 7, no. 4 (2016): 2842–2855.
- 21. C. Y. Chung, S. P. Li, K. K. W. Lo, and V. W. W. Yam, "Synthesis and Electrochemical, Photophysical, and Self-Assembly Studies on Water-Soluble pH-Responsive Alkynylplatinum(II) Terpyridine Complexes," *Inorganic Chemistry* 55, no. 9 (2016): 4650–4663.
- 22. T. R. Cook and P. J. Stang, "Recent Developments in the Preparation and Chemistry of Metallacycles and Metallacages via Coordination," *Chemical Reviews* 115, no. 15 (2015): 7001–7045.
- 23. Y. Y. Zhang, W. X. Gao, L. Lin, and G. X. Jin, "Recent Advances in the Construction and Applications of Heterometallic Macrocycles and Cages," *Coordination Chemistry Reviews* 344 (2017): 323–344.
- 24. J. Park, A. N. Pasupathy, J. I. Goldsmith, et al., "Coulomb Blockade and the Kondo Effect in Single-Atom Transistors," *Nature* 417, no. 6890 (2002): 722–725.
- 25. W. Chen, M. D. Fu, W. H. Tseng, et al., "Conductance and Stochastic Switching of Ligand-Supported Linear Chains of Metal Atoms," *Angewandte Chemie International Edition* 45, no. 35 (2006): 5814–5818.
- 26. 'M. G. Campbell, D. C. Powers, J. Raynaud, et al., "Synthesis and Structure of Solution-Stable One-dimensional Palladium Wires," *Nature Chemistry* 3, no. 12 (2011): 949–953.
- 27. S. Kundu, S. J. George, and G. U. Kulkarni, "Electric Field Assisted Assembly of 1D Supramolecular Nanofibres for Enhanced Supercapacitive Performance," *Journal of Materials Chemistry A* 8, no. 26 (2020): 13106–13113.
- 28. Y. Ma, W. Zhao, P. She, et al., "Electric Field Induced Molecular Assemblies Showing Different Nanostructures and Distinct Emission Colors," *Small Methods* 3, no. 7 (2019): 1900142.
- 29. Z. M. Hudson, C. Sun, K. J. Harris, B. E. Lucier, R. W. Schurko, and S. Wang, "Probing the Structural Origins of Vapochromism of a Triarylboron-Functionalized Platinum(II) Acetylide by Optical and Multinuclear Solid-State NMR Spectroscopy," *Inorganic Chemistry* 50, no. 8 (2011): 3447–3457.

Supporting Information

Additional supporting information can be found online in the Supporting Information section.

Supporting file: agt270088-sup-0001-SupMat.docx **Supporting file:** agt270088-sup-0001-SupMat.zip